THE JOURNAL OF BIOLOGICAL CHEMISTRY VOL. 287, NO. 3, pp. 2156–2167, January 13, 2012
© 2012 by The American Society for Biochemistry and Molecular Biology, Inc. Published in the U.S.A.

Generation and Functional Characterization of Knock-in Mice Harboring the Cardiac Troponin I-R21C Mutation Associated with Hypertrophic Cardiomyopathy*

Received for publication, August 16, 2011, and in revised form, November 14, 2011 Published, JBC Papers in Press, November 15, 2011, DOI 10.1074/jbc.M111.294306

Yingcai Wang[‡], Jose Renato Pinto[‡], Raquel Sancho Solis[§], David Dweck[‡], Jingsheng Liang[‡], Zoraida Diaz-Perez[‡], Ying Ge[§], Jeffery W. Walker[§¶†], and James D. Potter[‡1]

From the [‡]Department of Molecular and Cellular Pharmacology, University of Miami, Miller School of Medicine, Miami, Florida 33136, the [§]Human Proteomics Program and Department of Physiology, School of Medicine and Public Health, University of Wisconsin, Madison, Wisconsin 53706, and the [¶]Department of Physiology, University of Arizona, Tucson, Arizona 88724

Background: The R21C substitution in cardiac troponin I (cTnI) is associated with hypertrophic cardiomyopathy in man.
Results: The R21C mutation disrupts the consensus sequence for cTnI phosphorylation.
Conclusion: The KI mouse model showed remarkable degree of cardiac hypertrophy and fibrosis after 12 months of age.
Significance: One of the physiological roles for the phosphorylation of the cTnI N-terminal extension is to prevent cardiac hypertrophy.

The R21C substitution in cardiac troponin I (cTnI) is the only identified mutation within its unique N-terminal extension that is associated with hypertrophic cardiomyopathy (HCM) in man. Particularly, this mutation is located in the consensus sequence for β-adrenergic-activated protein kinase A (PKA)-mediated phosphorylation. The mechanisms by which this mutation leads to heart disease are still unclear. Therefore, we generated cTnI knock-in mouse models carrying an R21C mutation to evaluate the resultant functional consequences. Measuring the *in vivo* levels of incorporated mutant and WT cTnI, and their basal phosphorylation levels by top-down mass spectrometry demonstrated: 1) a dominant-negative effect such that, the R21C+/− hearts incorporated 24.9% of the mutant cTnI within the myofilament; and 2) the R21C mutation abolished the *in vivo* phosphorylation of Ser^{23}/Ser^{24} in the mutant cTnI. Adult heterozygous (R21C+/−) and homozygous (R21C+/+) mutant mice activated the fetal gene program and developed a remarkable degree of cardiac hypertrophy and fibrosis. Investigation of cardiac skinned fibers isolated from WT and heterozygous mice revealed that the WT cTnI was completely phosphorylated at Ser^{23}/Ser^{24} unless the mice were pre-treated with propranolol. After propranolol treatment (−PKA), the *p*Ca-tension relationships of all three mice (*i.e.* WT, R21C+/−, and R21C+/+) were essentially the same. However, after treatment with propranolol and PKA, the R21C cTnI mutation reduced (R21C+/−) or abolished (R21C+/+) the well known decrease in the Ca^{2+} sensitivity of tension that accompanies Ser^{23}/Ser^{24} cTnI phosphorylation. Altogether, the combined effects of the R21C mutation appear to contribute toward the development of HCM and suggest that another physiological role for the phosphorylation of Ser^{23}/Ser^{24} in cTnI is to prevent cardiac hypertrophy.

Hypertrophic cardiomyopathy (HCM)[2] is an autosomal dominant disease of the heart that has been linked to mutations in genes that encode at least 10 sarcomeric proteins (1–5). Some of these proteins make up the thin filament, a multimeric structure that performs both calcium-dependent and -independent roles in muscle contractility (6, 7). Within the thin filament, troponin I (TnI), troponin C (TnC), and troponin T (TnT) form the troponin (Tn) complex, which is responsible for switching on contraction and propagating the calcium-induced signal to the rest of the thin filament (6, 8). On calcium binding to Tn, a series of allosteric conformational changes occur, including the release of TnI inhibition, which promotes the interaction between actin and myosin required to generate force (9). Through the *in vitro* investigation of over 100 thick and thin filament mutations, it has become evident that the manifestation of pathological cardiomyopathies involves many complex processes such that these mutations intricately alter the calcium regulation of actomyosin-ATPase activity (7, 10).

All TnI isoforms share a high degree of plasticity that provides TnI the ability to adapt suitable conformations with TnC, TnT, and actin-tropomyosin in the presence and absence of calcium (9, 11, 12). Notably, cardiac TnI (cTnI) is different from the fast and slow skeletal TnI isoforms because it has an additional ~30 amino acids in its N terminus (9, 11, 12). The recent emergence of >60% of the crystal structure of cardiac Tn (cTn) has revealed and confirmed how the many subunit interactions join together to make up the cTn core domain (13). Despite these advances, there is a lack of information in the literature

---

* This work was supported, in whole or in part, by National Institutes of Health Grants HL042325 (to J. D. P.), RO1 HL081386 (to J. W. W.), 1K99HL103840-01 and J&E King Grant 10KN-13 (to J. R. P.), the Wisconsin Partnership Fund for a Healthy Future, and an American Heart Association Scientist Development Grant (to Y. G.).

[†] Deceased.

[1] To whom correspondence should be addressed: 1600 NW 10th Ave. (R-189), Miami, FL 33136. Fax: 305-243-4555; E-mail: jdpotter@miami.edu.

[2] The abbreviations used are: HCM, hypertrophic cardiomyopathy; cTn, cardiac troponin; cTnI, cardiac troponin I; cTnT, cardiac troponin T; cTnC, cardiac troponin C; R21C+/−, heterozygous animal; R21C+/+, homozygous animal; MHC, myosin heavy chain; tk, thymidine kinase; Ab, antibody; KI, knock-in mice; TDMS, top-down mass spectrometry; *p*Ca, −log [Ca^{2+}]$_{free}$; ES, embryonic stem.

pertaining to the structure of the cTnI N-terminal extension. Specifically, this portion of cTnI has not been resolved in structural studies due to its predicted flexibility (13). Within this N-terminal extension, two serines are present at positions 23 and 24 (including the initial methionine) that upon β-adrenergic stimulation of the heart, protein kinase A (PKA) becomes activated and phosphorylates them (14).

The N-terminal extension of cTnI has several biological functions that serve to maintain cardiac physiology under low and high demands of adrenergic stimulation. Deletion of cTnI residues 2–26 in a transgenic mouse model facilitated the diastolic and systolic functions of both young and aged hearts (15, 16). Furthermore, it has been shown that phosphorylation within the cTnI N-terminal extension: 1) increases the rate of relaxation and cross-bridge cycling kinetics (17–19); and 2) decreases both the Ca^{2+} affinity of cTnC (20) and the Ca^{2+} sensitivity of force generation (19). Altogether, these reports indicate that a major role for the cTnI N-terminal extension is to assist in the lusitropic effects of cardiac muscle relaxation (14).

Approximately 35 mutations in cTnI have been associated with hypertrophic, dilated, and restrictive cardiomyopathies (21). Among these, the R21C mutation is the only identified HCM-associated mutation located within the N-terminal extension of cTnI (22). A significant aspect of this mutation is that it is located within a PKA substrate consensus sequence (RRRSS) (23). Our previous *in vitro* studies showed that the R21C cTnI mutation reduced the level of PKA-mediated cTnI phosphorylation in reconstituted skinned fibers and curtails the well characterized decrease in the Ca^{2+} sensitivity of contraction associated with cTnI phosphorylation (24). Therefore, our focus shifted on generating and characterizing heterozygous and homozygous R21C cTnI knock-in (KI) mouse models in which one could investigate how the availability of phosphorylated cTnI contributes to the HCM phenotype. In a series of biochemical and proteomic assays, we investigated the ratio of mutant to wild-type cTnI protein incorporated into the mouse myofilament and their corresponding basal levels of phosphorylated cTnI. Irrespective of the mutant gene dosage, both the heterozygous (R21C+/−) and homozygous (R21C+/+) KI mice developed the HCM phenotype as evidenced by the presence of cardiac hypertrophy and fibrosis. Our results suggest that under circumstances where β-adrenergic stimulation occurs, limiting the lusitropic effects via the incomplete phosphorylation of cTnI may play a role in the development of the cardiac hypertrophic response.

EXPERIMENTAL PROCEDURES

Construction of Targeting Vector

A genomic clone including the entire murine *TNNI*3 was isolated from the mouse 129/sv genomic library (Stratagene). To construct the targeting vector (Fig. 1), two separate gene fragments were subcloned into two pBluescript II KS(+) vectors (Stratagene, La Jolla, CA): 1) the ClaI/XhoI 2.1-kb fragment containing exons 1–3 was used to generate the R/C mutation at codon 21. The mutation was introduced into a HindII/XhoI subclone containing exons 1–3 using the four-pair oligonucleotide PCR mutagenesis method. The sense oligonucleotide (5′-TGTCCGATGCCGC*T*CCTCTGCCAACTAC-3′) and antisense oligonucleotide (5′-AGTTGGCAGAGGAGC*A*GCGTCGGACAGGA-3′) contained the mutation (underlined) and the T7 and T3 primers were from the vector flanks. The PCR product was digested with HindII/XhoI to replace the same fragment in subclone 1. 2) The 4.8-kb XhoI/HindIII fragment encompasses exons 4–8. The targeting construct was generated in the vector Osdupdel, which contains MCI *neo* flanked by loxP and thymidine kinase (*tk*) under control of 3′-phosphoglycerate kinase (a gift from O. Smithies, University of North Carolina) by ligating the ClaI/XhoI fragment from plasmid 1 into the targeting vector downstream from the *neo* gene to form a 5′ homology region. The XhoI/HindIII fragment from plasmid 2 was ligated to the targeting vector between the *neo* and *tk* genes to form the 3′ homology region. The transcriptional orientation of *TNNI*3 and *neo* are opposite in this targeting vector.

Generation of cTnI Mutant Mice

Thirty micrograms of the NotI linearized construct was electroporated into Tc1 embryonic stem (ES) cells (25, 26). Culture and selection of recombinant ES clones were performed as described previously (27). Recombinant ES clones were screened by PCR with a 5′ primer located upstream of the ClaI site, which is located externally of the construct; and a 3′ primer from the *neo* gene, which amplifies a 2.5-kb fragment. Clones deemed positive by PCR were confirmed by Southern blot by digesting the DNA with SacI and probing it with 5′ and *neo* probes (see Fig. 1). This analysis was also verified with HindIII-digested DNA using a 3′ probe (Fig. 1). The same analyses were also used for the screening of heterozygous and homozygous mice. Three independent ES cell clones that carried the homologous recombinant construct were injected into C57BL/6 blastocysts. Male progeny with a high percentage of coat color chimerism were bred to C57BL/6 females to establish germ line transmission. Heterozygous mice were mated with CMV-Cre transgenic mice to delete the *neo* marker. The mouse genotypes were identified by PCR utilizing a pair of primers (P1 and P2) flanking the *neo* cassette (Fig. 1).

Northern Blot

Hearts were removed from the progeny and total RNA was extracted by using TRIzol reagent (Invitrogen). 15 μg of RNA were loaded onto a 1.0% agarose gel. After transfer, the blot was serially hybridized to probes, which were labeled with $[\alpha\text{-}^{32}\mathrm{P}]$dCTP by using the Rediprimer labeling kit (Amersham Biosciences). After each hybridization, the bound probe was removed by washing the blot with a boiling solution of 0.15 M NaCl, 0.15 M sodium citrate, 0.1% SDS, pH 7.0 (1× SSC, 0.1% SDS). Removal of the probes was confirmed before performing the next hybridization.

PCR and RT-PCR Analysis

PCR Analysis—To confirm the removal of the *neo* cassette in the *neo* recombinant allele, a fragment was amplified from the DNA of mouse tails by PCR using a pair of primers (5′-CTGAGCGTAGTGGTTAGCAGTGA and 5′-ACTGCGACCTCATCTACACCTTCAACTG) flanking the cTnI region in which the *neo* cassette was inserted. The PCR program was as follows: 1 cycle of 94 °C for 3 min, 35 cycles of 94 °C for 30 s, 56 °C for 45 s, and 72 °C for 90 s followed by one cycle of 72 °C for 5 min.

RT-PCR Analysis—Total RNA was extracted from heart tissue using TRIzol reagent (Invitrogen). cDNA was synthesized from 2 μg of total RNA from mouse ventricular tissue utilizing the OmniScript® RT Kit (Qiagen). Primers sets were designed from mouse cDNA sequences as follows: 5′-ATGGGCTCCTTCTCCATCA-3′ and 5′-AATGTGACCAAGCTGGTGAC-3 for atrial natriuretic peptide; 5′-ATGGATCTCCTGAAGGTGCT-3′ and 5′-AAGAGGGCAGATCTATCGGA-3′ for brain natriuretic peptide; 5′-CTGCTGCAGAGGTTATTCCTCG-3′ and 5′-GGAAGAGTGAGCGGCGCATCAAGG-3′ for α-myosin heavy chain (α-MHC); 5′-TGCAAAGGCTCCAGGTCTGAGGGC-3′ and 5′-GCCAACACCAACCTGTCCAAGTTC-3′ for β-myosin heavy chain (β-MHC); 5′-GCTTCACCACCTTCTTG-3′ and 5′-TCACCATCTTCCAGGAG-3′ for glyceraldehyde 3-phosphate dehydrogenase (GAPDH).

Myofibrillar Preparation and Phosphorylation Detection

Enriched myofibrillar proteins were isolated using F60 buffer (60 mM KCl, 30 mM imidazole, 7.2 mM MgCl$_2$, pH 7.0) containing protease and phosphatase inhibitor mixtures (Roche Diagnostics, catalog numbers 11836153001 and 05892791001) as previously described (28).

Detection by Pro-Q Staining—20 μg of myofibrils were loaded onto a 15% SDS-PAGE gel and phosphorylated proteins were detected with the Molecular Probes Pro-Q Diamond phosphoprotein gel stain reagent (Invitrogen, catalog number P-33301) as described in the manufacturer's manual. The total protein was further detected in the same gel using SYPRO Ruby staining. A transilluminator was then used to view and photograph the gel.

Detection by Antibodies—After running on a 15% SDS-PAGE, proteins were transferred to a polyvinylidene difluoride membrane (PVDF) and then incubated with antibodies: 22B11 (Research Diagnostics Inc., anti-cTnI specific for cTnI that is dephosphorylated at both Ser^{23} and Ser^{24}), mAb14 (MMS-4182, from Covance, CA, anti-cTnI, which detects cTnI that is phosphorylated at Ser^{24} independent of Ser^{23} phosphorylation status), and 6F9 (Research Diagnostics Inc., anti-cTnI raised against residues 189–195, which detects the total cTnI irrespective of Ser^{23}/Ser^{24} phosphorylation status). Immunoreactivity was detected using goat anti-mouse IgG labeled with Alexa 680 fluorophore (Rockland) at 1:2000 dilution. The reaction signal was developed and detected with an Odyssey Infrared imager (LI-COR).

Time Course of cTnI PKA Phosphorylation—Freshly isolated myofibrils were incubated for 30 or 60 min at 30 °C in 100 μl of 20 mM Tris-HCl (pH 7.0), 150 mM NaCl, 20 mM MgCl$_2$, 10 μM ATP, and 0.5 units/μl of the PKA catalytic subunit (Sigma, catalog number P2645). The reaction was stopped by the addition of Laemmli loading buffer (29) and boiled for 5 min. PKA inhibitor PKI 6–22 (Amide; Calbiochem) was used for control studies. The reaction contained 2 μg of myofibrils, which were used for Western blot analysis.

High Resolution Top-down Electron Capture Dissociation Mass Spectrometry in Mutant Mice

The troponin complex was purified from Triton X-100-skinned myofibrils by using affinity chromatography as described previously (30). Briefly, frozen mouse ventricular tissue (propranolol treated as below) was partially thawed, minced with a razor blade, and homogenized at maximum speed in a Polytron for 4–6 s in ice-cold relaxing solution (100 mM KCl, 10 mM imidazole (pH 7.0), 6 mM MgCl$_2$, 2 mM EGTA, 5 mM ATP, 1 mM PMSF, 1 mM DTT, 10 mM benzamidine, and 0.75 mg/ml of protease inhibitor mixture). The homogenized tissue was centrifuged at 500 × *g* (2 min) and the pellet was resuspended in 5 volumes of 0.33% Triton X-100, 0.5 mg/ml of BSA for 4 min at room temperature. This was followed by rinsing the pellet twice in relaxing solution to remove Triton X-100 and then incubating it for 1 h at 4 °C in extraction solution (0.7 M LiCl, 25 mM Tris (pH 7.5), 5 mM EGTA, 0.1 mM CaCl$_2$, 5 mM DTT, 1 mM PMSF, and 0.75 mg/ml of protease inhibitor mixture).

Troponin was affinity purified from the supernatant using Sepharose CL-4B-conjugated MF4 anti-cTnI monoclonal antibody (Hytest, Finland) after centrifugation of the extract at 10,000 × *g* for 45 min to remove cell debris. Bound troponin was eluted from the affinity resin with 50 mM glycine (pH 2) (adjusted with HCl), neutralized with MOPS (pH 9.0) buffer, and desalted on a C18 protein microtrap (Michrom Bioresources, Inc.). Top-down mass spectrometry (TDMS) was performed on a 7-tesla LTQ-FT-ICR Ultra (Thermo Scientific Inc., Bremen, Germany). Samples were introduced with a Triversa NanoMate (Advion BioSciences, Ithaca, NY) into the ESI source with a spray voltage of 1.4–1.6 kV and flow rate of 50–100 nl/min. Resolving power on the mass analyzer was set to 200,000 and acquisition scan rate of 1 scan/s. Data were analyzed with Manual Xtract and Xcalibur software (Thermo Scientific) based on the mouse cTnI protein sequence obtained from the Swiss-Prot database (accession number P48787). Reported M_r values are the most abundant masses. Further details on mass spectrometry analysis can be found in Refs. 30 and 31.

Microscopy

Mice were sacrificed by exposure to CO$_2$. Heart/body weight was first measured to determine whether hypertrophy had occurred. The hearts were fixed in 10% formalin overnight or longer at 4 °C, then embedded and stained with hematoxylin-eosin or Masson trichrome. Light microscopic images were recorded digitally with an Axiovert 200 microscope (10 × 40). Wild-type, heterozygous mutant (R21C+/−), and homozygous mutant (R21C+/+) animals were age matched for all studies.

Cardiac Skinned Fiber Preparation

The mice were sacrificed using two different protocols approved by the animal care and use committee (IACUC) at the University of Miami. The mice were exposed to CO$_2$ followed by cervical dislocation; or they were first anesthetized with isoflurane, then injected intravenously with propranolol (1 mg/kg body weight, Calbiochem, catalog number 537075), and 30 min later were given another exposure to isoflurane before cervical

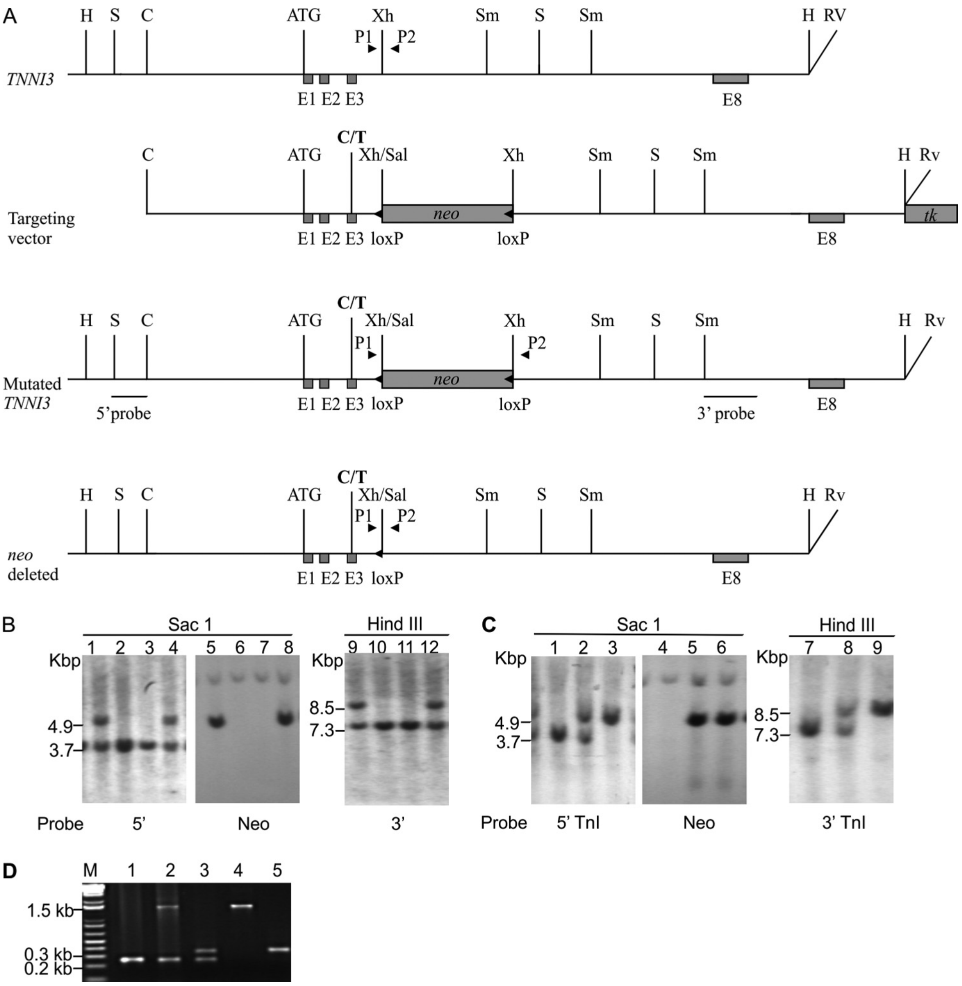
A
TNNI3
H S C ATG Xh Sm S Sm H RV
P1 P2
E1 E2 E3 E8
Targeting vector
C ATG C/T Xh/Sal Xh Sm S Sm H Rv
neo tk
E1 E2 E3 loxP loxP E8
Mutated TNNI3
H S C ATG C/T Xh/Sal Xh Sm S Sm H Rv
P1 P2
neo
5'probe E1 E2 E3 loxP loxP 3' probe E8
neo deleted
H S C ATG C/T Xh/Sal Sm S Sm H Rv
P1 P2
E1 E2 E3 loxP E8
B
Sac 1
Hind III
1 2 3 4 5 6 7 8 9 10 11 12
Kbp
4.9
3.7
8.5
7.3
Probe 5' Neo 3'
C
Sac 1
Hind III
1 2 3 4 5 6 7 8 9
Kbp
4.9
3.7
8.5
7.3
Probe 5' TnI Neo 3' TnI
D
M 1 2 3 4 5
1.5 kb
0.3 kb
0.2 kb

FIGURE 1. **Gene targeting: mutation of the mouse cTnI gene.** *A*, diagram from the top to the bottom shows: *wild type TNNI3,* the exon-intron organization and simplified restriction map of the murine *TNNI3* gene; *targeting vector,* the targeted construct region to introduce the loxP flanked *neo* cassette, *tk* gene, and the R21C mutation; *mutated TNNI3,* the mutated *TNNI3* gene after homologous recombination and the probes used for Southern blotting to identify the targeted ES cell clone and the mutated mice; *neo deleted,* the R21C mutation in the targeted *TNNI3* gene after *neo* deletion. Restriction sites: *C*, ClaI; *H*, HindIII; *Rv*, EcoRV; *S*, Sac1; *Sal*, SalI; *Sm*, SmaI; *Xh*, XhoI. *B*, Southern blot showing the targeted and untargeted ES cell clones after SacI digestion using the 5′ cTnI and *neo* probes, and after HindIII digestion using the 3′ cTnI probe. *Lanes 1*, *4*, *5*, *8*, *9*, and *12* are targeted ES clones and *2*, *3*, *6*, *7*, *10*, and *11* are untargeted ES clones. Note that digestion of targeted DNA generates fragments that are 1.2-kb bigger than the wild-type DNA due to the inclusion of the 1.2-kb *neo* cassette in the targeted DNA allele. *C*, Southern blot analysis of SacI- and HindIII-digested tail DNA of progeny from interheterozygote mating. *Lanes 1*, *4*, and *7*, wild type; *2*, *5*, and *8* are heterozygote (*neo*+/−); *lanes 3*, *6*, and *9* are homozygote (*neo*+/+). *D*, PCR analysis showing the *neo* gene deletion in tail DNA from the offspring of mated *neo*+/− mice with EIIa-Cre mice. Note that the *neo* cassette (1.2 kb) was deleted, but one loxP site remained in the sequence, which is evidenced by the presence of the additional 33 bp (loxP site) in the targeted allele; *lane 1*, wild-type; *lanes 2* and *3*, heterozygote before and after *neo* removal, respectively; *lanes 4* and *5*, homozygote before and after *neo* deletion, respectively.

dislocation. The hearts were excised, and the left ventricles were dissected. Cardiac muscle fibers were prepared and mounted following a standard laboratory procedure (32).

Measurement of Calcium Dependence of Force Development

The Ca^{2+} dependence of force development and maximal force were determined before and after a 30-min PKA incubation according to Baudenbacher *et al.* (32).

Statistical Analyses

All data are presented as mean ± S.E. One-way analysis of variance followed by Dunnett or Student-Newman-Keuls tests was used to determine the significance between groups.

RESULTS

Generation and Characterization of cTnI Mutant Mice—The R21C cTnI mutant mice were generated using a knock-out/knock-in strategy (26, 27). Fig. 1*A* illustrates the gene targeting strategy used to generate a C to T point mutation in the *TNNI3* gene, which corresponds to changing Arg (CGC) in codon 21 of exon 3 to Cys (TGC). The point mutation was introduced into a targeting construct containing a floxed *neo* cassette within intron 3. Other than this mutation, the coding sequence in the construct including the entire 8 exons of the *TNNI3* gene was unchanged. The targeting construct was linearized with NotI and electroporated into 129/SV-derived Tc1 embryonic stem cells.

The recombinant ES cell clone cultivation and selection were performed as described in the literature (26, 27). The positive ES clones containing the R21C+/− mutation in the *TNNI3* gene were first characterized by digesting ES cell-derived DNA with SacI and probing it with 5′ *TNNI3* and *neo* probes; and then confirmed using a 3′ probe against HindIII-digested DNA (Fig. 1*B*). Because a 1.2-kb *neo* cassette was inserted into intron

3 of the *TNNI3* gene, the mutant allele generated a band that is 1.2 kb larger than the wild-type allele when digested by either SacI or HindIII.

Two independent R21C+/− positive ES clones were injected into C57BL/6 blastocysts to produce male chimeras. These males were mated with C57BL/6 females to obtain heterozygotes (*i.e.* one allele carrying the R21C mutation and the *neo* cassette, referred here as *neo*+/−), and cross-mating inter-heterozygous *neo*+/− mice resulted in the generation of homozygotes (*i.e.* both alleles carrying the R21C mutation and *neo* cassette, referred to here as *neo*+/+). The *neo*+/− and *neo*+/+ mice were identified by Southern blots of tail DNA using the same panel of digestion enzymes and probes as described for screening the recombinant ES cells (Fig. 1*C*).

The phenotypes of *TNNI3*-targeted mice from the two independently derived ES clones were identical. Deletion of the *neo* cassette was performed by mating *neo*+/− mice to CMV-Cre "deleter" transgenic mice, which resulted in the R21C cTnI heterozygous mutant (*i.e.* one allele carrying the R21C mutation without the *neo* cassette, referred here as R21C+/−), and cross-mating inter-heterozygous R21C+/− mice resulted in the generation of R21C homozygous mice (*i.e.* both alleles carrying the R21C mutation without the *neo* cassette, referred to as R21C+/+). Upon activation of the Cre recombinase, the *neo* cassette was expected to be removed and leave a single loxP site (33 bp in length) within the targeted allele. Fig. 1*D* shows the amplification products from tail DNA by PCR using the P1 and P2 primer pair (see Fig. 1*A*) that flank the *neo* cassette within intron 3 of the *TNNI3* gene. Analysis of the amplification products yields a 1683-nucleotide band for the *neo* containing allele, a 250-nucleotide band for the wild-type allele, and a 283-nucleotide band for the *neo*-deleted allele. As anticipated, sequencing the DNA of R21C+/+ cTnI mice in the region adjoining the 5′ and 3′ homology region of the construct revealed that a single loxP sequence (33 bp) remained after Cre/loxP recombination (Fig. 1*D*, *lanes 3* and *5*). Sequencing the cTnI mRNA extracted from R21C+/+ mouse hearts confirmed that it was identical to the wild-type mRNA with the exception of the C-T mutation at codon 21.

The phenotype of the *neo*+/− mice was indistinguishable from the wild-type mice; whereas, the *neo*+/+ mice exhibited a lethal phenotype that is very similar to the previously reported targeted loss-of-function mutation in cTnI (33). The *neo*+/+ mice were born healthy with morphologically normal hearts; however, they all died of acute heart failure 18–20 days after birth. Northern and Western blot analysis revealed that these mice lacked the expression of cTnI mRNA and protein in the heart (data not shown). The deletion of the *neo* cassette by mating the *neo*+/− mice with CMV-Cre transgenic mice generated the R21C+/− and R21C+/+ mice. The R21C+/+ mice displayed a new distinctive phenotype compared with the *neo*+/+ mice because they were viable, fertile, and lived at least 18 months. These results suggest that the *neo* cassette interfered with proper splicing of the cTnI transcript from the recombined gene. However, subsequent removal of the *neo* cassette from the recombined gene resulted in the lethal phenotype to be rescued and the distinctive HCM phenotype to predominate in the R21C+/+ mutant mice when aged greater than 12 months.

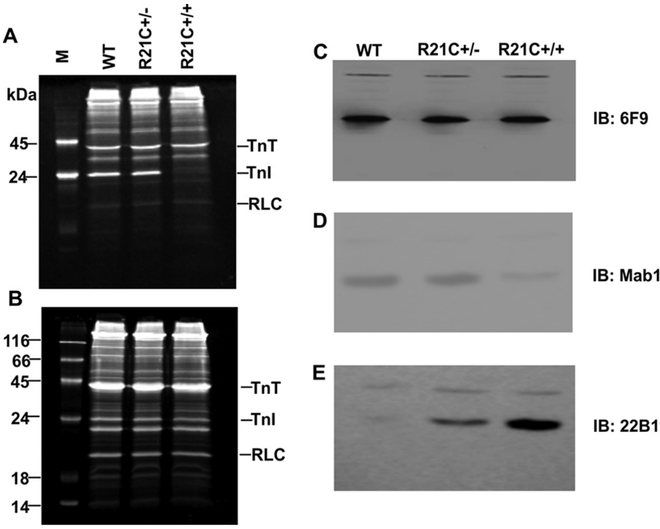

FIGURE 2. **Detection of total, phosphorylated, and dephosphorylated cTnI in myofibrils isolated from WT, R21C+/−, and R21C+/+ nonpropranolol-treated murine hearts.** *A*, 15% SDS-PAGE stained with Pro-Q diamond to detect phosphorylated cardiac myofibrilar proteins. *B*, 15% SDS-PAGE gel stained with SYPRO Ruby to reveal the total cardiac myofibrilar protein contents. *C*, Western blot (*IB*) analysis showing the total cTnI in cardiac myofibrils (total cTnI is calculated by defining the WT band intensity stained by the 6F9 AB as 100%). *D*, Western blot analysis showing the phosphorylated cTnI (phosphorylated cTnI is calculated by defining the WT band intensity stained by mAb14 as 100%). *E*, Western blot analysis showing the dephosphorylated cTnI (dephosphorylated cTnI is calculated by defining the R21C+/+ band intensity stained by the 22B11 Ab as 100%). All myofibrils were prepared from murine hearts that were not injected with propranolol.

One of the limitations of this work was the use of an animal with a mixed background. The R21C mutant and WT mice were generated from crossing 129/sv mice with C57BL/6 mice. Recently it was reported that the C57BL/6J strain can maintain cardiac function better than most of the inbred strains after *ex vivo* ischemia, including 129/sv. However, during *in vivo* acute hypoxia, the 129/sv mice maintained close to normal cardiac function, whereas the C57BL/6J animals showed dramatic cardiac decompensation (34). In this work, we are unable to address whether a particular background would develop a more pronounced or diminished phenotype.

Alteration of cTnI Protein Phosphorylation in R21C Mutant Mice—Our previous *in vitro* studies showed a significantly slower rate of PKA-mediated phosphorylation of human recombinant R21C cTnI compared with the WT cTnI (24). Largely based on our previous results, we decided to further investigate the status of cTnI phosphorylation in the mutant mice. Therefore, myofibrils were prepared from the left ventricles of 2-month-old KI mice and evaluated for protein phosphorylation using a Pro-Q Diamond phosphoprotein gel, which employs a noncovalent fluorescent dye that selectively stains phosphoproteins on polyacrylamide gels. Fig. 2*A* shows that the amount of phosphorylated cTnI is nearly undetectable in R21C+/+ mice. Nevertheless, the level of other phosphoproteins, such as cTnT and myosin regulatory light chain remained unchanged in both the R21C+/+ and R21C+/− mutant mice when compared with the WT mice (Fig. 2*A*). The cTnI and regulatory light chain were identified in the gel accordingly (35)

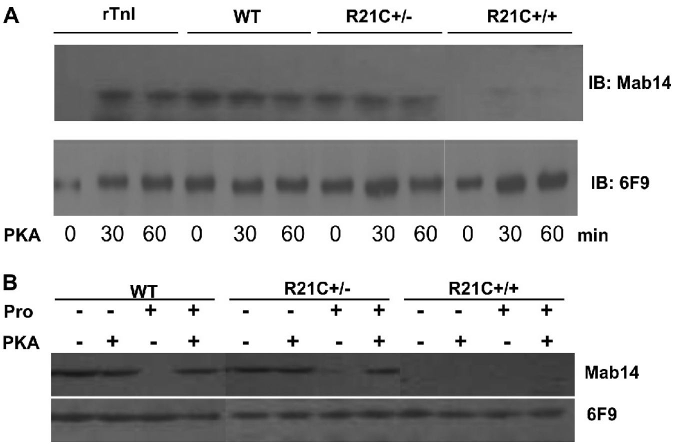

FIGURE 3. **Western blot analysis of cTnI phosphorylation after PKA treatment.** *A*, recombinant cTnI (rTnI) and myofibrils from WT, R21C+/−, and R21C+/+ mouse hearts were treated with PKA at different times (0–60 min). *Upper panel* shows the immunoblot (*IB*) of cTnI with the mAb14 antibody (detects phosphorylated cTnI) and the *lower panel* shows the immunoblot of cTnI with the 6F9 antibody (detects total cTnI). *B*, immunoblot analysis using mAb14 and 6F9 antibodies in skinned fibers in the presence and absence of propranolol (Pro) and PKA.

and the cTnT was identified as a band that co-migrates at the same level as actin. The same gel was stained using SYPRO Ruby to measure the total protein content. Among all three types of mice (*i.e.* WT, R21C+/+, and R21C+/−), no differences in the expression of cTnI or other myofibrilar proteins were found (Fig. 2*B*).

To quantify the phosphorylation of Ser^{23} and Ser^{24} in cTnI from all three types of mice, the following three antibodies (Ab) were used for Western blot analysis: 1) 6F9, a mAb that equally detects the phosphorylated and dephosphorylated cTnI; 2) mAb14, a monoclonal Ab that recognizes cTnI phosphorylated at Ser^{24} independent of Ser^{23} phosphorylation; and 3) 22B11, a monoclonal Ab that recognizes cTnI only if Ser^{23} and Ser^{24} are both dephosphorylated. Fig. 2*C* shows that the total amount of cTnI incorporated into the thin filaments of the WT, R21C+/+, and R21C+/− mice remained unchanged. However, the amount of phosphorylated cTnI in R21C+/+ mutant hearts was nearly abolished in comparison to the WT mice (Fig. 2*D*). The amount of dephosphorylated cTnI (Fig. 2*E*) is seemingly inversely proportional to the levels of phosphorylated cTnI (Fig. 2, *D* and *E*). Dephosphorylated cTnI was undetectable in the WT mice and increased in a mutant gene dose-dependent manner (Fig. 2*E*). It is worthwhile mentioning that the Arg-Cys substitution could disrupt the mAb14 antibody binding epitope; however, the mass spectrometry data (Fig. 4) presented below corroborates the Western blotting data, which illustrates that R21C+/+ cTnI is not phosphorylated.

Fig. 3*A* shows the effect of PKA addition on the phosphorylation of cTnI in the absence of propranolol pretreatment. Skinned muscle (*i.e.* myofibrils) prepared from ventricles were incubated with PKA for 30 and 60 min at room temperature and then analyzed by Western blot using mAb14 and the 6F9 Ab (described above) to detect phosphorylated and total cTnI, respectively. Fig. 3*A* shows that at all time points (*i.e.* 0, 30, and 60 min) the cTnI was completely phosphorylated in myofibrils isolated from WT and R21C+/− mice. To determine whether the complete phosphorylation of cTnI (WT and R21C+/−) may be due to the method by which the animals were sacrificed, other methods of sacrificing were pursued, such as anesthesia with isoflurane or ether followed by cervical dislocation. Independent of the manner by which the animals were sacrificed, all the data indicated that the cTnI from the WT and R21C+/− mice was completely phosphorylated (data not shown). In efforts to prevent the *in vivo* phosphorylation of cTnI, the animals were injected with propranolol to block β-adrenergic stimulation of endogenous PKA before sacrificing. Fig. 3*B* is a Western blot that shows that phosphorylated cTnI is undetectable in skinned fibers from WT and R21C+/− mice that were injected with propranolol. Moreover, Fig. 3*B* shows that after exogenously adding PKA to the skinned fibers, the cTnI became completely phosphorylated after 30 min. These results indicate that the cTnI from the WT and R21C+/− myofibrils were already completely phosphorylated before the addition of exogenous PKA *in vitro*; therefore, further phosphorylation of cTnI cannot occur upon exogenous PKA treatment. In contrast, phosphorylated cTnI from R21C+/+ mouse myofibrils were nearly undetectable before and after PKA treatment (Fig. 3*A*). Although the level of cTnI phosphorylation could be manipulated by administering propranolol, the levels of phosphorylated cTnT and regulatory light chain 2 remained unchanged when the mice were treated with propranolol and incubated with PKA (see Fig. 2*A*).

Determination of R21C cTnI Incorporation into the Thin Filament of Mutant Mice—Fig. 4 shows the analysis of affinity purified cTn heterotrimer complexes subjected to TDMS. The proteins were extracted from skinned myofibrils and purified as whole troponin complexes; therefore, the cTnI species detected by mass spectrometry represent the proteins as they are incorporated *in vivo* within the thin filament. Fig. 4*A* illustrates representative spectra of the different cTnI species derived from R21C+/−, R21C+/+, and WT animals. A peak with a mass of 24155.7 Da was unique to the homozygous knock-in mice (Fig. 4*A*, *middle panel*) and ECD fragmentation produced 12 *z*-ion fragments (data not shown) consistent with the C-terminal sequence of mouse cTnI. R21C+/− animals showed this peak superimposed on an apparently normal wild-type pattern of cTnI peaks (30, 31) including a mass of 24168.8 Da for unphosphorylated, 24248.8 Da for monophosphorylated, and 24328.8 Da for biphosphorylated forms (Fig. 4*A*, *top* and *bottom panels*). The intensity ratios of the different cTnI species from the R21C+/− animals were 24.9, 50.3, 21.4, and 3.4% for mutant unphosphorylated cTnI, WT un-, WT mono-, and WT biphosphorylated cTnI forms, respectively (Fig. 4*B*, *left graph*). The intensity ratios of the WT cTnI species from the WT mice were 67.5, 29.3, and 3.3% for un-, mono-, and biphosphorylated forms, respectively (Fig. 4*C*). Notably, this relatively low level of cTnI phosphorylation reflects the use of propranolol to minimize the impact of β-adrenergic stimulation during the handling and sacrificing of the animals. Although a very small amount of mutant phosphorylated cTnI may exist, the mass spectra data suggests that it is statistically insignificant. In R21C+/−, the ratio of mutant to wild-type cTnI (including all phosphorylated forms) was about 1:3 (mutant:WT) (Fig. 4*B*, *right panel*).

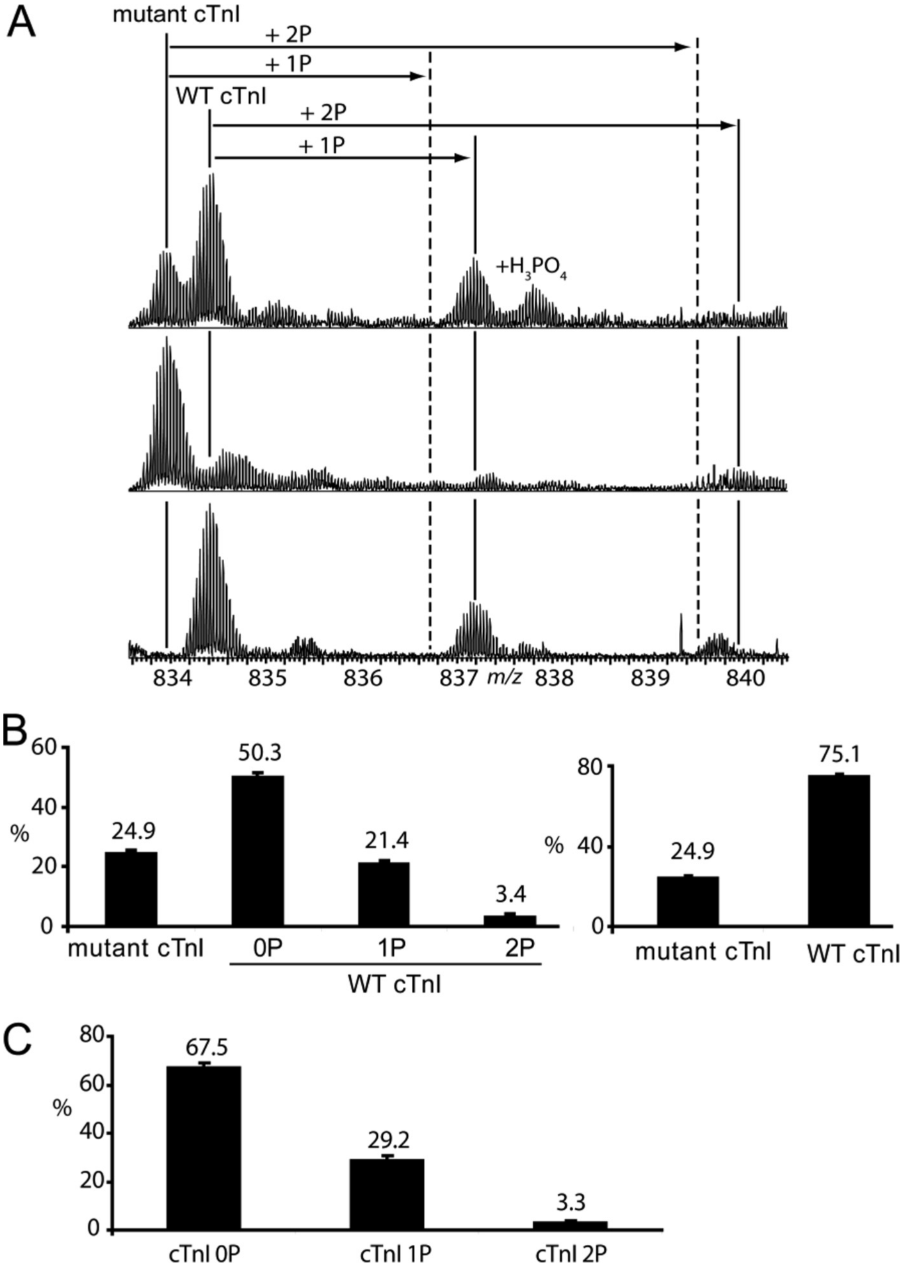

FIGURE 4. **Relative abundance of cTnI and phosphorylated cTnI in WT and R21C propranolol-treated mice.** *A*, ESI/FTMS spectrum of cTnI protein ions (*M29+*) in unphosphorylated (*0P*), monophosphorylated (*+1P*), and bisphosphorylated *(+2P)* states. *Top panel*, cTnI from a R21C+/− mouse; *middle panel*, cTnI from a R21C+/+ mouse; *bottom panel*, cTnI from a WT mouse. $+H_3PO_4$ (+98 Da) indicates a noncovalent phosphate adduct of unphosphorylated cTnI peaks. *B,* distribution of mutant and WT cTnI in un-, mono-, and bis-phosphorylated states (*left panel*); and ratio of the relative abundance of mutant and WT (all forms combined) cTnI (*right panel*) from an R21C+/− mouse heart ($n = 10$ charge states analyzed). *C*, ratio of the relative abundance of unphosphorylated (*0P*), monophosphorylated (*+1P*), and bisphosphorylated (*+2P*) cTnI in WT mice. *Bar graphs* represent an average of five experiments with errors reported as mean ± S.E.

R21C Mutant Mice Display Cardiac Hypertrophy—The R21C mutant mice were investigated for evidence of altered cardiac morphology, such as hypertrophy. With regard to the heart/body weight ratio and histology in R21C mutant mice, no significant differences were observed at 3- and 6-month-old mice when compared with WT mice (data not shown). However, Figs. 5 and 6 show that after 12 months of age, the R21C mutant mice exhibited all of the hallmarks of HCM. The heart/body weight ratio was significantly increased in the older mice (Fig. 5*A*). Moreover, the RNA expression of some well conserved markers of cardiac hypertrophy were markedly elevated in the hearts of 18-month-old R21C mutant mice compared with the age-matched WT mice. Respectively, the R21C+/− and R21C+/+ mice increased the expression of atrial natriuretic peptide 3.82- and 4.28-fold; brain natriuretic peptide 3.3- and 3.68-fold; and β-MHC 2.85- and 3.0-fold (Fig. 5, *B* and *C*). The expression of the hypertrophic markers was evaluated at 3, 6, 9, 12, and 18 months of age. No significant differences were observed in 3–6-month-old R21C mutant mice when compared with the WT mice. The expression levels started to increase at 9 months; and the peak was achieved at 12 months (data not shown). Consistent with the elevation of the afore-

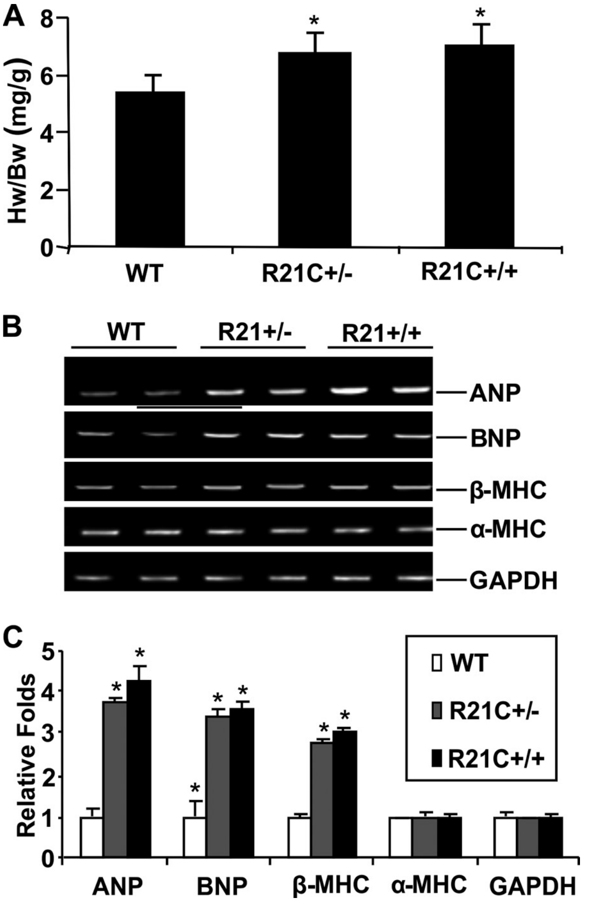

FIGURE 5. **Heart/body weight ratio and expression of molecular markers of cardiac hypertrophy.** *A*, heart/body weight ratio of 18-month-old WT, R21C+/−, and R21C+/+ mice. *B*, total RNA from heart extracts of 18-month-old mice that were analyzed by RT-PCR. *ANP*, atrial natriuretic peptide; *BNP*, brain natriuretic peptide; and *GAPDH*, glyceraldehyde 3-phosphate dehydrogenase are indicated. *C*, quantitative analysis of the RT-PCR measured by band densitometry. Densitometric analyses are representative of at least 3 independent experiments; and the figure depicts the fold gene up-regulation in the mutant mice compared with the same genes expressed in the WT mice.

mentioned cardiac hypertrophic molecular markers, characteristic morphological features associated with HCM were also observed, such as a significant increase in the left ventricle outer and septal wall thickness (Fig. 6*A*) and pronounced interstitial fibrosis (Fig. 6*B*).

The Calcium Sensitivity of Force Development in Skinned Fibers—Our previous *in vitro* studies using reconstituted cardiac skinned fibers showed that the R21C mutation causes several functional consequences including, an increase in the Ca^{2+} sensitivity of force and impairment of PKA-treated skinned fibers to decrease the Ca^{2+} sensitivity of contraction (24). Therefore, we investigated the Ca^{2+} sensitivity of contraction in skinned fibers using homogeneous systems derived from R21C KI mice. Fig. 7 shows the Ca^{2+} sensitivity of force development of cardiac fibers that were either isolated from mice treated with or without propranolol prior to sacrificing, followed by either an *in vitro* treatment with or without PKA. The rationale for such experiments was to determine whether the R21C mutation and the levels of phosphorylated cTnI within the mutant myofilament are mutually exclusive events with respect to changing the Ca^{2+} sensitivity of contraction in skinned fibers.

Table 1 summarizes the $p\mathrm{Ca}_{50}$ ($-\log\ [\mathrm{Ca}^{2+}]_{\mathrm{Free}}$ that produces 50% of the maximal response), Hill coefficient, and recovered maximal force from the experiments illustrated in Fig. 7. In the absence of considerable levels of phosphorylated cTnI (as shown in Fig. 3), the $p\mathrm{Ca}_{50}$ of the WT, R21C+/−, and R21C+/+ fibers were all similar (Table 1, group A). These results suggest that at low to undetectable levels of phosphorylated cTnI, the mutant gene dosage does not contribute to large changes in Ca^{2+} sensitivity.

Initially, our experiments were set up to compare Ca^{2+} sensitivities of PKA-treated and non-PKA-treated fibers. However, during the course of our investigation, we realized that regardless of whether or not the fibers were treated with PKA, the WT and heterozygous fibers all had similar levels of phosphorylated cTnI (see Fig. 2*D*). Thereby, indicating that the fibers were already fully phosphorylated *in vivo*, before PKA treatment. To circumvent this issue and determine how the activation of PKA affects the Ca^{2+} sensitivity of contraction in WT and mutant fibers, mice were treated with propranolol to attain baseline (*i.e.* nonphosphorylated) Ca^{2+} sensitivities and then compared with fibers treated with propranolol and PKA (*i.e.* phosphorylated).

Table 1 shows that when WT mice were treated with propranolol and subsequently, the fibers were incubated with PKA (group C), the calcium sensitivity reduced 0.25 *p*Ca units in comparison to the baseline WT fibers (group A). These results confirm that significant reductions in the Ca^{2+} sensitivity of contraction occur due to the activation of PKA. However, the R21C+/− fibers incubated with PKA (group C) reduced the calcium sensitivity to a lesser extent (−0.14 *p*Ca units) when compared with the un-treated R21C+/− fibers (group A). Interestingly, the R21C+/+ fibers nearly completely blunted the decrease in Ca^{2+} sensitivity (−0.05 *p*Ca units) associated with PKA-mediated cTnI phosphorylation (see Table 1, groups A and C). Altogether, these results suggest that the R21C mutation reduces the PKA accessibility to phosphorylate cTnI and blunts the anticipated decrease in myofilament Ca^{2+} sensitivity in a mutant gene dosage-dependent manner.

The n_{Hill} (Hill coefficient, an index of thin filament cooperativity) was also analyzed in all four groups. Only the propranolol-treated R21C+/− fibers in group A were significantly increased in comparison to the WT fibers in group A (Table 1). However, homozygous fibers that were phosphorylated (*i.e.* groups B, C, and D) all showed a significant decrease in the n_{Hill} compared with WT of each respective group. The maximal force was significantly decreased in all fibers from groups B, C, and D (*i.e.* in the presence of *in vivo* and/or *in vitro* cTnI phosphorylation) when compared with their respective fibers treated with propranolol in the absence of PKA (Group A). However, the maximal force was not significantly altered among the WT, R21C+/−, and R21C+/+ mice within the same groups (Table 1).

DISCUSSION

The "poison peptide" hypothesis asserts that the incorporation of mutant proteins within the sarcomere exerts a domi-

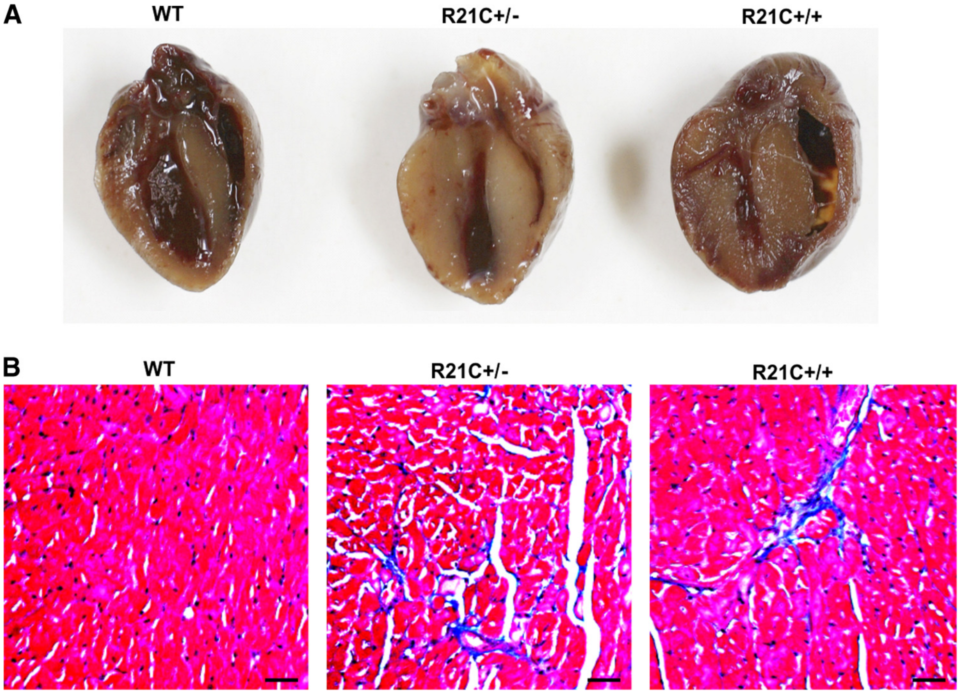

FIGURE 6. **Histopathology of knock-in mouse hearts.** *A*, sections of 18-month-old hearts murine showing hypertrophy of the left ventricle and septal wall in R21C mutant mice. *B*, cross-sections of the left ventricle stained with Masson trichrome showing interstitial fibrosis and myofibrilar disarray in R21C mutant mice (*bars* = 100 μm).

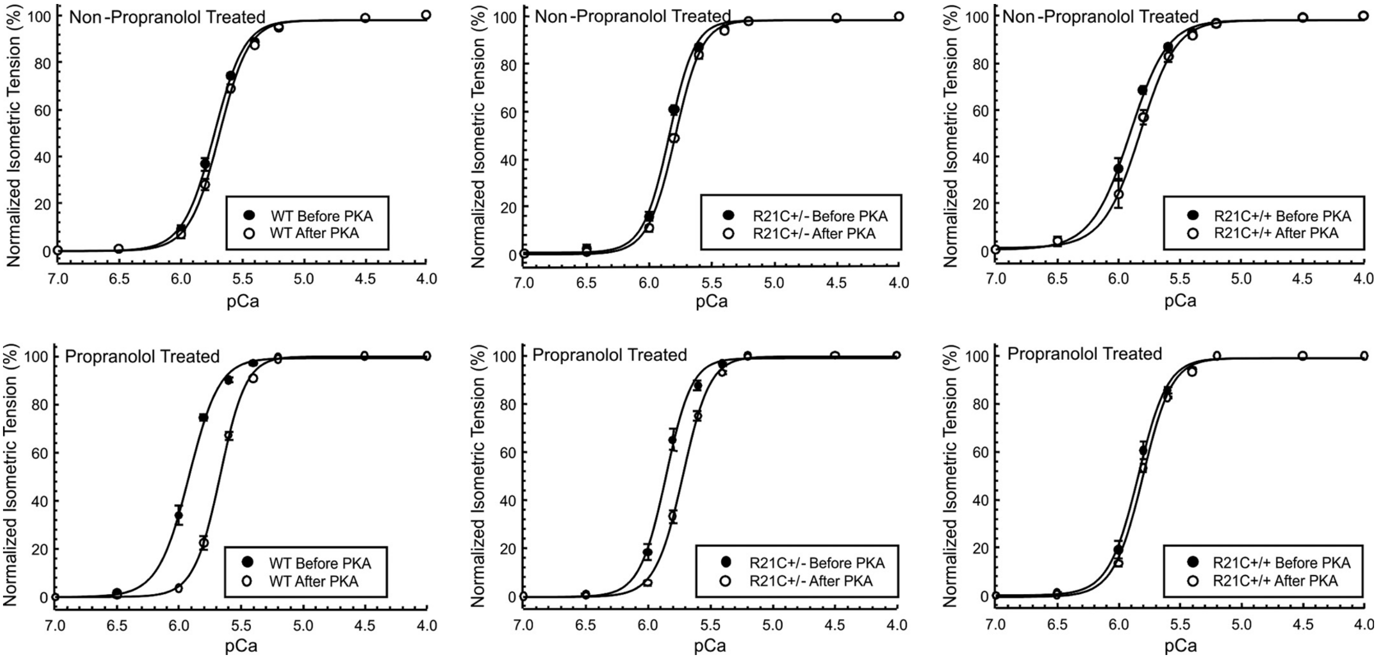

FIGURE 7. **Effect of PKA phosphorylation on the Ca^{2+} sensitivity of force development in cardiac skinned fibers.** *Top panels*, Ca^{2+} sensitivity of force development before and after PKA incubation in the nonpropranolol-treated animals. *Bottom panels*, Ca^{2+} sensitivity of force development before and after PKA incubation in the propranolol-treated animals. Each *curve* represents an average of four to eight experiments with errors reported as mean ± S.E.

nant-negative effect that leads to dynamic molecular and structural changes associated with the diseased phenotype (36). It is expected that the expression of the mutant protein is incorporated up to 50% within the myofilament because most of the individuals carrying the mutation are heterozygous. However, the expression of mutant proteins often goes unmeasured and the precise incorporation of R21C cTnI in patients is unknown. Generally, estimates of the ratio of mutant to WT protein incorporation have mainly been indirect through quantifying the RNA expression of mutant transcripts and/or Western blotting techniques (37, 38). However, the advent of TDMS has provided a precise and useful tool to measure the *in vivo* ratios of mutant and WT cTnI proteins and their phosphorylation levels in novel KI mouse models of HCM (30, 31).

Cardiac myofibrils isolated from R21C+/− cTnI mice incorporated both the WT and mutant forms of cTnI. Such a side by

TABLE 1

Effects of PKA phosphorylation on the Ca^{2+} sensitivity of force development in knock-in R21C cardiac skinned fibers

Data are shown as the mean ± S.E.

Fiber genotype	Before PKA treatment[a]			After PKA treatment[b]			No. experiments
	pCa_{50}	n_{Hill}	Maximal force	pCa_{50}	n_{Hill}	Maximal force	
			KN/m²			*KN/m²*	
	Propranolol (group A)[c]			Propranolol (group C)[c]			
WT	5.92 ± 0.02	3.56 ± 0.17	57.66 ± 2.14	5.67 ± 0.02^{d}	4.17 ± 0.18^{d}	49.45 ± 2.15^{d}	4
R21C+/−	5.88 ± 0.02	4.19 ± 0.11^{e}	57.14 ± 2.89	$5.74 \pm 0.01^{e,f}$	3.99 ± 0.13	52.06 ± 2.74^{f}	4
R21C+/+	5.87 ± 0.01^{e}	3.70 ± 0.17	56.91 ± 2.30	$5.82 \pm 0.01^{e,g,h}$	3.68 ± 0.11	52.49 ± 1.37^{h}	4
	Non-propranolol (group B)[i]			Non-propranolol (group D)[i]			
WT	5.73 ± 0.01^{d}	3.60 ± 0.17	51.91 ± 1.59^{d}	5.70 ± 0.01^{d}	3.69 ± 0.15	48.18 ± 1.65^{d}	10
R21C+/−	$5.84 \pm 0.01^{e,f}$	4.30 ± 0.26	54.22 ± 1.11	$5.79 \pm 0.01^{e,f}$	4.14 ± 0.26	50.34 ± 1.42^{f}	9
R21C+/+	$5.92 \pm 0.03^{e,g}$	2.93 ± 0.29^{g}	52.59 ± 1.67^{h}	$5.86 \pm 0.02^{e,g}$	3.11 ± 0.41^{g}	49.60 ± 1.44^{h}	6

[a] Muscle fibers not treated with PKA after dissection.
[b] Muscle fibers treated with PKA after dissection.
[c] Baseline group in which animals were injected with propranolol to limit β-adrenergic activation prior to sacrificing.
[d] $p < 0.05$, WT within group A *versus* WT within groups B, C, and D.
[e] $p < 0.05$, WT *versus* R21C+/− or R21C+/+ within the same group.
[f] $p < 0.05$, R21C+/− within a group A *versus* R21C+/− within groups B, C, and D.
[g] $p < 0.05$, R21C+/− *versus* the R21C+/+ within the same group.
[h] $p < 0.05$, R21C+/+ within group A *versus* R21C+/+ within groups B, C, and D.
[i] Animals not injected with propranolol prior to sacrificing.

side comparison of cTnI proteins expressed in the same genotypic heart revealed that: 1) the overall expression of the mutant cTnI was ~25% of the total expression of the protein; 2) the WT cTnI was basally phosphorylated at Ser^{23}/Ser^{24}; and 3) phosphorylated R21C cTnI was undetectable (Figs. 3 and 4). Although phosphorylation of cTnI by PKC can occur at Ser^{43}/Ser^{45} and Thr^{144}, which decreases the myofilament Ca^{2+} sensitivity (18, 39, 40), our results coincide with previous studies (31), which show that serines 23 and 24 are the only two sites basally phosphorylated *in vivo* within the WT murine cTnI protein. These findings suggest that one or more of the following may occur in the murine heart: 1) phosphorylation of Ser^{23}/Ser^{24} is dominant over the phosphorylation of Ser^{43}/Ser^{45} and Thr^{144} and/or 2) PKC-mediated phosphorylation of cTnI does not increase as a compensatory mechanism for the decrease in PKA-mediated phosphorylation.

A characteristic PKA consensus motif, "RRRSS" exists in the human, cow, rabbit, and rodent cTnI. At least two basic residues at −2 and −3 positions are required to allow phosphorylation of the serine at position 0 by PKA (41). The Ser^{23}/Ser^{24} residues in R21C cTnI fulfills this requirement and this partial sequence is called a duplicated minimal recognition PKA motif (42). This suggests that Arg^{21} is a crucial residue for PKA to recognize and phosphorylate this serine cluster because the phosphorylation of Ser^{23}/Ser^{24} in R21C+/+ myofibrils was undetected by TDMS and Pro-Q Diamond staining (Figs. 3 and 4). In support of this hypothesis, *in vitro* studies have shown that the recombinant R21C cTnI protein in the troponin complex is phosphorylated by PKA at a significantly slower rate than the wild-type (24).

Both the R21C hetero- and homozygous mice developed hallmark traits associated with HCM, such as, increasing: 1) the heart to body weight ratio (Fig. 5*A*); 2) the expression of hypertrophic molecular markers (Fig. 5*B*); 3) the left ventricular and septal wall thickness (Fig. 6*A*); 4) interstitial fibrosis (Fig. 6*B*); and 5) myofibrilar disarray (Fig. 6*B*). The severity of the HCM phenotype does not seem to be dependent on the R21C mutant gene dosage because ~25% of the total cTnI is mutated in the heterozygotes and is sufficient to promote a similar hypertrophic response to that of the homozygous mice. Nevertheless, previous studies have shown that an increase in the ratio of mutant to WT protein *in vivo* and *in vitro* within myofilaments can lead to larger phenotypic and/or lethal effects (43). Therefore, *in vivo* hemodynamic and echocardiographic parameters of the R21C KI mice will have to be examined to clearly determine whether the mutant gene dosage alters the severity of the R21C HCM phenotype in mice.

Recent reports have demonstrated via TDMS that the phosphorylation status of cTnI may be a credible biomarker for the early detection of mild to severe hypertrophy and dilation (44). Postmortem heart tissue samples from normal and severely affected patients showed that ~56 and 1% of the total cTnI was phosphorylated, respectfully (44). Other studies have also shown that phosphorylated cTnI is lower in heart failure patients (45–47) by using phosphate affinity SDS-PAGE to separate the phosphorylated species of cTnI. For example, Messer *et al.* (45) demonstrated that in the donor heart samples, the bisphosphorylated species predominated (72.2%); whereas, in diseased hearts, the dephosphorylated species of cTnI predominated (~77%). Notably, phosphorylation of Ser^{43} and Thr^{142} (corresponding to Thr^{144} in murine cTnI) were not detected in human donor samples. Based on the above, a decrease in the level of phosphorylated WT cTnI from 32.5% in the WT mice to 24.5% in the heterozygous R21C+/− mice (Fig. 4) may also be attributed to activation of the hypertrophic response.

At least three mechanisms seem to contribute to reduction in the level of phosphorylated cTnI in the R21C+/− KI mice. First, the R21C mutation in cTnI may disrupt the PKA consensus motif, rendering the mutant incapable of *in vivo* phosphorylation; second, the mutant indirectly reduces the available WT cTnI that can be phosphorylated (16); last, the cardiomyocyte may respond by reducing the physiological levels of phosphorylated cTnI. The existence of all three mechanisms imply that although the heterozygous mice express 75% of the WT cTnI, the mutant poison peptide exerts a dominant-negative effect that reduces the available levels of WT cTnI that can be phosphorylated. In support of this hypothesis, a transgenic animal that simultaneously expresses a nonphosphorylatable deletion mutant of cTnI (Δ2–26) and the full-length WT cTnI significantly lowered the level of phosphorylated WT CTnI when compared with nontransgenic mice (16).

Several transgenic mouse models have been generated to elucidate the physiological role of PKA phosphorylation on cTnI. Among the PKA targets in the heart, cTnI is considered a key regulatory protein that increases the rate of muscle relaxation and contributes to the shortening of the cardiac twitch during β-adrenergic stimulation (12, 17, 19). A transgenic mouse model lacking the PKA phosphorylation sites (*i.e.* Ser^{23}/Ser^{24} to alanine) or lacking both the PKA and PKC phosphorylation sites (*i.e.* Ser^{43}/Ser^{45} and Thr^{144}) did not respond by decreasing the Ca^{2+} sensitivity of contraction upon treatment with PKA; whereas, the WT mice decreased their *p*Ca-tension relationship 0.28 *p*Ca units (48, 49). Furthermore, Kentish *et al.* (17) have shown that overexpression of slow skeletal TnI, which lacks the N-terminal domain, did not decrease the myofilament Ca^{2+} sensitivity upon PKA treatment. Their results suggest that PKA-mediated relaxation (*i.e.* decrease in Ca^{2+} sensitivity and increase in rate of relaxation) are mainly due to the phosphorylation of cTnI.

Current paradigms related to cardiomyopathy suggest that mutations associated with HCM tend to increase the myofilament Ca^{2+} sensitivity; whereas, mutations associated with dilated cardiomyopathy tend to decrease the myofilament Ca^{2+} sensitivity (10). Moreover, these paradigms emerged as a result of investigating the effects of mutations in the absence of cTnI phosphorylation. For example, the following HCM-associated mutations in cTnI all increase the Ca^{2+} sensitivity of force development in skinned fibers: R145G, R145Q, R162W, S199N, and Δ183 (3, 50). In contrast, the *p*Ca-tension relationship of fibers isolated from R21C+/− and R21C+/+ KI mice were essentially the same as the WT mice when they were all pretreated with propranolol (group A, Table 1). However, upon PKA activation (group C, Table 1), the pCa_{50} values of the R21C+/+ and R21C+/− fibers decreased 0.15 and 0.07 log units, respectively, in comparison to the WT fibers (Table 1, group C). Currently, the results presented herein do not seem to contradict the paradigms because after cTnI phosphorylation, the R21C+/+ myofilament is not desensitized to calcium and maintains a higher Ca^{2+} sensitivity of contraction than the WT fibers.

Although our Pro-Q diamond staining results suggests that the phosphorylation levels of CTnT, regulatory light chain, and other myofilament proteins (Fig. 2*A*) in the R21C mice are not different from the WT levels, it is worthwhile mentioning that this technique is better suited for qualitative rather than quantitative measurements. This suggests that small changes in the levels of phosphorylated myofilament proteins can occur and go undetected by gel staining procedures. Nevertheless, our TDMS data showed that the R21C+/− mice reduced their basal levels of phosphorylated cTnI by 8% when compared with the WT mice.

The pCa_{50} values arising from phosphorylated WT, R21C+/−, and R21C+/+ fibers (*i.e.* Table 1, groups B, C, and D) were not identical. This suggests that other mechanisms independent of cTnI phosphorylation may contribute to changing the Ca^{2+} sensitivity of force. This rationale stems from the notion that *in vivo* PKA activity is tightly regulated by the β-adrenergic pathway, which integrates many PKA modulators up- and downstream of its targets; whereas, in skinned muscle preparations, many of these regulators are missing.

At least one of the molecular mechanisms by which the R21C mutation causes cardiac disease is through impairing the ability of cTnI to be phosphorylated by PKA, consequently decreasing the myofilament response to β-adrenergic stimulation. Surprisingly, when reduced levels of cTnI phosphorylation (*i.e.* propranolol treated) prevail, the Ca^{2+} sensitivity of contraction for the WT and mutant fibers were similar, suggesting that the mutation and phosphorylation levels of cTnI are mutually exclusive with regard to changing the myofilament Ca^{2+} sensitivity. Rather, evidence supporting the poison peptide hypothesis arises when the myofilaments are phosphorylated. Based on this rationale, a small (in R21C+/− mice) and large (R21C+/+ mice) reduction in the level of cTnI phosphorylation is sufficient to change the myofilament Ca^{2+} sensitivity, which may lead to a remarkable degree of cardiac hypertrophy, fibrosis, and activation of the fetal gene program, which all contribute to abnormal contractility and the development of heart disease.

Acknowledgments—We thank Dr. Shen Li for technical assistance in mouse surgical experiments and Dr. Harada for providing the original clone for the murine cTnI genomic DNA.

REFERENCES

1. Kimura, A., Harada, H., Park, J. E., Nishi, H., Satoh, M., Takahashi, M., Hiroi, S., Sasaoka, T., Ohbuchi, N., Nakamura, T., Koyanagi, T., Hwang, T. H., Choo, J. A., Chung, K. S., Hasegawa, A., Nagai, R., Okazaki, O., Nakamura, H., Matsuzaki, M., Sakamoto, T., Toshima, H., Koga, Y., Imaizumi, T., and Sasazuki, T. (1997) *Nat. Genet.* **16,** 379–382
2. Mogensen, J., Klausen, I. C., Pedersen, A. K., Egeblad, H., Bross, P., Kruse, T. A., Gregersen, N., Hansen, P. S., Baandrup, U., and Borglum, A. D. (1999) *J. Clin. Invest.* **103,** R39–R43
3. Gomes, A. V., and Potter, J. D. (2004) *Mol. Cell. Biochem.* **263,** 99–114
4. Liew, C. C., and Dzau, V. J. (2004) *Nat. Rev. Genet.* **5,** 811–825
5. Konno, T., Chang, S., Seidman, J. G., and Seidman, C. E. (2010) *Curr. Opin. Cardiol.* **5,** 205–209
6. Gordon, A. M., Homsher, E., and Regnier, M. (2000) *Physiol. Rev.* **80,** 853–924
7. Tardiff, J. C. (2011) *Circ. Res.* **108,** 765–782
8. Marston, S. B., and Redwood, C. S. (2003) *Circ. Res.* **93,** 1170–1178
9. Perry, S. V. (1999) *Mol. Cell. Biochem.* **190,** 9–32
10. Willott, R. H., Gomes, A. V., Chang, A. N., Parvatiyar, M. S., Pinto, J. R., and Potter, J. D. (2010) *J. Mol. Cell Cardiol.* **48,** 882–892
11. Day, S. M., Westfall, M. V., and Metzger, J. M. (2007) *J. Mol. Med.* **85,** 911–921
12. Layland, J., Solaro, R. J., and Shah, A. M. (2005) *Cardiovasc. Res.* **66,** 12–21
13. Takeda, S., Yamashita, A., Maeda, K., and Maéda, Y. (2003) *Nature* **424,** 35–41
14. Kranias, E. G., and Solaro, R. J. (1982) *Nature* **298,** 182–184
15. Barbato, J. C., Huang, Q. Q., Hossain, M. M., Bond, M., and Jin, J. P. (2005) *J. Biol. Chem.* **280,** 6602–6609
16. Biesiadecki, B. J., Tachampa, K., Yuan, C., Jin, J. P., de Tombe, P. P., and Solaro, R. J. (2010) *J. Biol. Chem.* **285,** 19688–19698
17. Kentish, J. C., McCloskey, D. T., Layland, J., Palmer, S., Leiden, J. M., Martin, A. F., and Solaro, R. J. (2001) *Circ. Res.* **88,** 1059–1065
18. Noland, T. A., Jr., Guo, X., Raynor, R. L., Jideama, N. M., Averyhart-Fullard, V., Solaro, R. J., and Kuo, J. F. (1995) *J. Biol. Chem.* **270,** 25445–25454

19. Zhang, R., Zhao, J., Mandveno, A., and Potter, J. D. (1995) *Circ. Res.* **76,** 1028–1035
20. Robertson, S. P., Johnson, J. D., Holroyde, M. J., Kranias, E. G., Potter, J. D., and Solaro, R. J. (1982) *J. Biol. Chem.* **257,** 260–263
21. Chang, A. N., Parvatiyar, M. S., and Potter, J. D. (2008) *Biochem. Biophys. Res. Commun.* **369,** 74–81
22. Arad, M., Penas-Lado, M., Monserrat, L., Maron, B. J., Sherrid, M., Ho, C. Y., Barr, S., Karim, A., Olson, T. M., Kamisago, M., Seidman, J. G., and Seidman, C. E. (2005) *Circulation* **112,** 2805–2811
23. Kennelly, P. J., and Krebs, E. G. (1991) *J. Biol. Chem.* **266,** 15555–15558
24. Gomes, A. V., Harada, K., and Potter, J. D. (2005) *J. Mol. Cell. Cardiol.* **39,** 754–765
25. Deng, C., Wynshaw-Boris, A., Zhou, F., Kuo, A., and Leder, P. (1996) *Cell* **84,** 911–921
26. Wang, Y., Szczesna-Cordary, D., Craig, R., Diaz-Perez, Z., Guzman, G., Miller, T., and Potter, J. D. (2007) *FASEB J.* **21,** 2205–2214
27. Wang, Y., Spatz, M. K., Kannan, K., Hayk, H., Avivi, A., Gorivodsky, M., Pines, M., Yayon, A., Lonai, P., and Givol, D. (1999) *Proc. Natl. Acad. Sci. U.S.A.* **96,** 4455–4460
28. Fewell, J. G., Hewett, T. E., Sanbe, A., Klevitsky, R., Hayes, E., Warshaw, D., Maughan, D., and Robbins, J. (1998) *J. Clin. Invest.* **101,** 2630–2639
29. Laemmli, U. K. (1970) *Nature* **227,** 680–685
30. Sancho Solis, R., Ge, Y., and Walker, J. W. (2008) *J. Muscle Res. Cell Motil.* **29,** 203–212
31. Ayaz-Guner, S., Zhang, J., Li, L., Walker, J. W., and Ge, Y. (2009) *Biochemistry* **48,** 8161–8170
32. Baudenbacher, F., Schober, T., Pinto, J. R., Sidorov, V. Y., Hilliard, F., Solaro, R. J., Potter, J. D., and Knollmann, B. C. (2008) *J. Clin. Invest.* **118,** 3893–3903
33. Huang, X., Pi, Y., Lee, K. J., Henkel, A. S., Gregg, R. G., Powers, P. A., and Walker, J. W. (1999) *Circ. Res.* **84,** 1–8
34. Barnabei, M. S., Palpant, N. J., and Metzger, J. M. (2010) *Physiol. Genomics* **42A**, 103–113
35. Monasky, M. M., Biesiadecki, B. J., and Janssen, P. M. (2010) *J. Mol. Cell. Cardiol.* **48,** 1023–1028
36. Marian, A. J., and Roberts, R. (1998) *Ann. Med.* **30,** Suppl. 1, 24–32
37. Wen, Y., Pinto, J. R., Gomes, A. V., Xu, Y., Wang, Y., Wang, Y., Potter, J. D., and Kerrick, W. G. (2008) *J. Biol. Chem.* **283,** 20484–20494
38. Wen, Y., Xu, Y., Wang, Y., Pinto, J. R., Potter, J. D., and Kerrick, W. G. (2009) *J. Mol. Biol.* **392,** 1158–1167
39. Burkart, E. M., Sumandea, M. P., Kobayashi, T., Nili, M., Martin, A. F., Homsher, E., and Solaro, R. J. (2003) *J. Biol. Chem.* **278,** 11265–11272
40. Takeishi, Y., Chu, G., Kirkpatrick, D. M., Li, Z., Wakasaki, H., Kranias, E. G., King, G. L., and Walsh, R. A. (1998) *J. Clin. Invest.* **102,** 72–78
41. Jaquet, K., Thieleczek, R., and Heilmeyer, L. M., Jr. (1995) *Eur. J. Biochem.* **231,** 486–490
42. Mittmann, K., Jaquet, K., and Heilmeyer, L. M., Jr. (1992) *FEBS Lett.* **302,** 133–137
43. Du, C. K., Morimoto, S., Nishii, K., Minakami, R., Ohta, M., Tadano, N., Lu, Q. W., Wang, Y. Y., Zhan, D. Y., Mochizuki, M., Kita, S., Miwa, Y., Takahashi-Yanaga, F., Iwamoto, T., Ohtsuki, I., and Sasaguri, T. (2007) *Circ. Res.* **101,** 185–194
44. Zhang, J., Guy, M. J., Norman, H. S., Chen, Y. C., Xu, Q., Dong, X., Guner, H., Wang, S., Kohmoto, T., Young, K. H., Moss, R. L., and Ge, Y. (2011) *J. Proteome Res.* **10,** 4054–4065
45. Messer, A. E., Gallon, C. E., McKenna, W. J., Dos Remedios, C. G., and Marston, S. B. (2009) *Proteomics Clin. Appl.* **3,** 1371–1382
46. Messer, A. E., Jacques, A. M., and Marston, S. B. (2007) *J. Mol. Cell. Cardiol.* **42,** 247–259
47. Bodor, G. S., Oakeley, A. E., Allen, P. D., Crimmins, D. L., Ladenson, J. H., and Anderson, P. A. (1997) *Circulation* **96,** 1495–1500
48. Pi, Y., Kemnitz, K. R., Zhang, D., Kranias, E. G., and Walker, J. W. (2002) *Circ. Res.* **90,** 649–656
49. Pi, Y., Zhang, D., Kemnitz, K. R., Wang, H., and Walker, J. W. (2003) *J. Physiol.* **552,** 845–857
50. Robinson, P., Griffiths, P. J., Watkins, H., and Redwood, C. S. (2007) *Circ. Res.* **101,** 1266–1273